

Main Paths of Brain Fibers in Diffusion Images Mixed with a Noise to Improve Performance of Tractography Algorithm-Evaluation in Phantom

Alireza Shirazinodeh¹, Hadis Faraji², Sam Sharifzadeh Javidi¹, Amir Homayoun Jafari^{3,4}, Mohammadreza Nazemzadeh^{4,5}, Hamidreza Saligheh Rad^{4,6*}

ABSTRACT

Background: Some voxels may alter the tractography results due to unintentional alteration of noises and other unwanted factors.

Objective: This study aimed to investigate the effect of local phase features on tractography results providing data are mixed by a Gaussian or random distribution noise.

Material and Methods: In this simulation study, a mask was firstly designed based on the local phase features to decrease false-negative and -positive tractography results. The local phase features are calculated according to the local structures of images, which can be zero-dimensional, meaning just one point (equivalent to noise in tractography algorithm), a line (equivalent to a simple fiber), or an edge (equivalent to structures more complex than a simple fiber). A digital phantom evaluated the feasibility current model with the maximum complexities of configurations in fibers, including crossing fibers. In this paper, the diffusion images were mixed separately by a Gaussian or random distribution noise in 2 forms: a zero-mean noise and a noise with a mean of data.

Results: The local mask eliminates the pixels of unfitted values with the main structures of images, due to noise or other interferer factors.

Conclusion: The local phase features of diffusion images are an innovative solution to determine principal diffusion directions.

Keywords

Diffusion Tractography; Diffusion Magnetic Resonance Imaging; Features; Gaussian Distribution; Local Phase; Noise; Feasibility Studies; Brain

Introduction

Diffusion in Magnetic Resonance Imaging (d-MRI), in forms of the diffusion tensor imaging [1] and high angular resolution diffusion imaging, such as q-ball [2] diffusion spectrum imaging [3] spherical de-convolution [4], and other novelty methods, is a technique based on movements of water molecules inside the tissues, including brain tissues [5]. The Difference in the diffusion of water molecules in the brain tissues reveals anatomical findings [6], and tractography detects the configurations of microstructures in the brain [7]. Resolu-

¹PhD Candidate, Department of Medical Physics and Biomedical Engineering, Medicine School, Tehran University of Medical Sciences, Tehran, Iran

²MSc, Research Center for Molecular and Cellular Imaging Advanced Medical Technologies and Equipment, Tehran University of Medical Sciences

³PhD, Research Center for Biomedical Technologies and Robotics (RCB-TR) Tehran University of Medical Sciences, Tehran, Iran

⁴PhD, Department of Medical Physics and Biomedical Engineering, Medicine School, Tehran University of Medical Sciences, Tehran, Iran

⁵PhD, Research Center for Molecular and Cellular Imaging Advanced Medical Technologies and Equipment, Tehran University of Medical Sciences, Tehran, Iran

⁶PhD, Quantitative Medical Imaging Systems Group, Research Center for Molecular and Cellular Imaging, Tehran University of Medical Sciences, Tehran, Iran

*Corresponding author: Hamidreza Saligheh Rad Quantitative Medical Imaging Systems Group, Research Center for Molecular and Cellular Imaging, Imam Khomeini Hospital, Keshavarz, Boulevard, Tehran, Iran
E-mail: hamid.h-salighehrad@tums.ac.ir

Received: 25 August 2021
Accepted: 27 January 2022

tion in diffusion data is high when diffusivity is high, which is desirable for clinical applications. D-MRI with higher spatial resolution can result in improving detection structures of the brain [8-12]. However, a major challenge for d-MRI is the intrinsically low signal-to-noise ratio (SNR), and increasing the SNR is caused due to decreasing b-value parameter, angular resolution declined related to the detection of microstructures. Sotiropoulos et al. [10] proposed a model of data based on combining high-spatial-resolution data with data of higher angular resolution and contrast to achieve benefits both.

Statistical model of signal and noise has an important effect on medical image analysis, and many applications in MRI are more sensitive when the data is well-defined based on a statistical model. In some types of researches, these methods are described as follows: 1) noise removal and signal estimation [13], 2) signal and noise maximum likelihood estimation [14], 3) linear minimum mean square error (LMMSE) filtering based schemes [15], or unbiased nonlocal mean filters [16].

The distribution of noise may also affect the results of image processing in MRI, and the effects of Rician noise on a coil are important for estimation of SNR and filtration of images especially in diffusion tensor estimation [15].

Averaging is another method to promote the SNR; for unreal data and less than threshold SNR, the prepared model cannot fit the signal by calculating the average of data mixed with correlated Gaussian noise [17].

The final goal in the acquisition of diffusion images is to determine the configurations of neurons in the structures of the brain with the tractography algorithm to predict diseases, such as Alzheimer's and epilepsy. Many researchers focused on the effectiveness of the tractography methods to predict the numbers and shapes of fibers passing through a voxel, also studied structural tractography and arrangement of nerve fibers based on internal structures obtained from data [1-6, 18]. Ad-

ditionally, the target could be a phantom or white matter of the human brain; the relationship between lines obtained from outputs of the tractography algorithms with actual fibers can be a question. Since the tractography algorithms are affected by parameters, such as noise, masks, and region of interest (ROI), selected by users according to the type of cases, small changes lead to incorrect findings. The connection index in the most possible tractography algorithms is a simple voxel count, which is a simple count [18]. Accordingly, these limitations lead to paths for reducing errors in the tractography algorithms.

The local structures of diffusion images considered a solution in all directions can lead to a more accurate estimation of the fibers. This paper aimed to promote tractography outputs in presence of noise.

In this paper, the pixels are addressed based on their property of the local frequency in all directions of diffusion signals. First, a digital phantom was selected based on the configurations of nerve fibers [19], and the images were in 60 directions using the local phase algorithm; the local frequency feature for all of the images was calculated. In the following, the value of each pixel was compared with the average of the total pixels of each image, and all pixels with smaller values than a threshold (mean of total pixels) were replaced with zero to design the desired mask. However, the address of non-zero pixels in the data is the same as their address in a mask, values of those pixels are just selected from data as the input of the tractography algorithm. Finally, the overall tracts of the fibers in the phantom were detected by the Hough transform [20].

Material and Methods

This simulation and analytical study aimed to examine the impact of the local phase features

on the tractography algorithm in noisy data. Some voxels may alter the tractography results due to unintentional alteration of noises

and other unwanted factors. Further, in the proposed method, the aim was to improve the output of the tractography algorithm in noisy images based on the local structures to select appropriate pixels and remove other pixels considered wrong selections of nerve fibers. This proposed technique employs the local structures of images along anatomical structures to investigate the brain fibers. Accordingly, the monogenic algorithm proposed by Felsberg et al. was used with the implementation of the local phase feature [21].

Local frequency as a feature of local phase

Implementation of Local frequency

A difference of Poisson filter (DOP) was used with $\lambda = 10$; the Poisson distribution is specified with one parameter: λ that equals the mean and variance. Increasing λ to sufficiently large values can lead to approximate the Poisson distribution by the normal distribution (λ) that λ was considered 10 since the distribution function of the designed filter has the least attenuation at intermediate frequencies (Figure 1).

The Fourier transform (in frequency domain) of the diffusion images was used in different directions and slices for given results as an input of Spherical Quadrature Filter. In the spatial domain, the procedure is as follows [22]:

$$p = (\text{diffusion images}) \otimes \text{DOP} \quad (1)$$

$$q = (\text{diffusion images}) \otimes [(i\cos\varnothing, isin\varnothing)\text{DOP}] \quad (2)$$

The symbol \otimes is the convolution in the spatial domain and DOP is a difference of Poisson filter. The local phase model is as follow, including the local frequency f_x :

$$r = \bar{\varnothing}(\cos\theta, \sin\theta)^T = \frac{q}{|q|} \arg(p + i|q|) \quad (3)$$

In Equation 3, r is obtained from a combination of directions and the local Phase. By using the derivative direction in the direction n_x to y ($\nabla = (\partial y_1, \partial y_2)$), we have:

$$f \triangleq (\nabla \bar{\varnothing})^T \cdot n = \frac{p \nabla^T q - q^T \nabla p}{p^2 + |q|^2}, n = [\cos(\theta), \sin(\theta)]^T \quad (4)$$

It was shown that the local frequency can be directly obtained by using the response of the four proposed filters.

Creating a mask using local frequency information

According to the previous section, a mask was designed with pixels introducing information about the local structure of the original image. This mask is multiplied by diffusion images to eliminate the values of some pixels in the tractography algorithm. In the case of Gaussian noise, we have:

$$\text{Mask}_{d,s}(x,y) = 0, \text{ if } (\text{local } f \text{ Matrix})_{d,s}(x,y) < (L_{\max} - \sigma), \text{ if not, Mask} = 1$$

$$L_{\max} = \max(\max((\text{local } f \text{ Matrix})_{d,s}(:, :))) \quad (5)$$

$$\sigma = \begin{cases} 0.1 < \sigma < 0.3 & \text{if for low SNR} \\ 0.3 < \sigma < 0.7 & \text{if SNR} \gg 1 \end{cases}$$

In the case of random noise $\sigma = 0$.

Here, the coordination of (x,y) indicates each pixel; $(\text{local } f \text{ Matrix})_{d,s}(x,y)$ is a value of each pixel based on a local frequency fea-

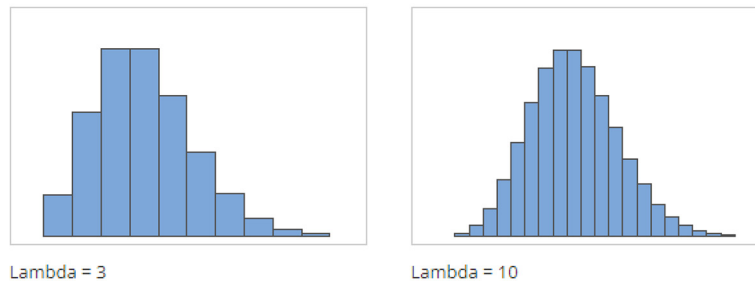


Figure 1: The distribution function of Poisson based on lambda parameter

ture of a pixel. (*local f Matrix*) $_{d,s}(:, :)$ is the local frequency matrix of a diffusion image in each slice and all directions; d and s indicate the direction and the slice number of each image, respectively. σ depends on SNR (Signal to Noise Ratio) and a parameter determining the lower band of the local structures in each image. Based on Equation 5, if the value under the Mask in each pixel is equal to one, this pixel is a candidate for the main structure of the image. Finally, the diffusion images are multiplied pixel by pixel with the local mask; therefore, only the pixels that represent the local changes are selected as the inputs of the tractography algorithm, and fiber bundles can be detected as the local structures in diffusion images.

$$I_{d,s}(x, y) = I_{d,s}(x, y) \langle \bullet \bullet \rangle \text{Mask}_{d,s}(x, y), \forall x, y, d, s \quad (6)$$

The Symbol $\langle \bullet \bullet \rangle$ is the pixel by pixel multiplication.

Hough Tractography

The Hough transform was used by Aganj as a tractography algorithm [20] that the brain fibers are modeled as 3D curves and parameterized with an arc length S . The aim is to obtain the value of each point x of the curve. First, it is assumed that the starting point of curve s has two-sides from each seed point, then the parametric line fits the curve as follow:

$$\bar{x}_s = \bar{x}_0 + \int_0^s t_s ds \quad (7)$$

which x_0 represents the starting point or the same as a seed point, and t_s represents the unit tangent vector at any point $(x, y, z)_s$ of curve S . Now, the coordinates of t_s is written in a spherical space.

$$t_s = \begin{pmatrix} x \\ y \\ z \end{pmatrix}_s \rightarrow \begin{pmatrix} \sin\theta \times \cos\phi \\ \sin\theta \times \sin\phi \\ \cos\theta \end{pmatrix}_s \quad (8)$$

The θ and ϕ are fitted with a polynomial in order of N . Using the Hough transform, the coefficients of each polynomial are calculated

based on available diffusion data. The desired fibers are selected to log-probability of the existence of fiber. The expression of probability is directly related to Generalized Fractional Anisotropy (GFA) inside the region of interest. In the current study, GFA was determined by the local phase mask, i.e. local mask represents the probability for the point located inside fiber bundles passing in each direction.

Noise Distributions

In this paper, the noise distributions added to d-MRI images are Gaussian and random as follow:

$$\text{Gaussian noise} = A\sqrt{v} \times \mu(K) + M \quad (9)$$

$$\text{Random noise} = A \times \mu(K); K = \text{size}(\text{data}) \quad (10)$$

In Equation 9 and 10, the amplitude of the noise is A , v is the variance of the noise, M is mean of data that correspond to mean of data, and $\mu(K)$ is a random function based on the size of data. In the case of Gaussian, two approaches are considered: the distribution of noise with zero mean and a certain mean as similar as the mean of data.

Results

Select the data type

The data was obtained from a digital phantom made by Leemans [23], and the image parameters are as follows:

6 non-DWIs ($b = 0$ s/mm²), 60 DWIs ($b = 1200$ s/mm²), voxel size = $1 \times 1 \times 1$ mm³ and SNR = INF (no noise added). Figure 2a and b show the phantom images and the results of the local phase model on the phantom images, respectively.

Results for a Gaussian noise

The Gaussian noise is firstly generated by the variance and mean of the data. The amplitude of the noise changed from upward to downward and added the modified noise to the diffusion images to reach multi SNR ranges.

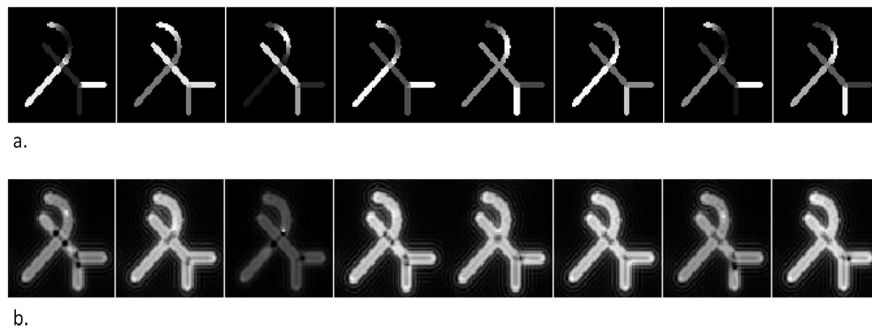


Figure 2: (a) A digital phantom (b) applying the Local phase algorithm on a digital phantom

In Figure 3, the left column is the orientation distribution function (ODF) of the digital phantom when the local phase mask was applied and the middle column showed the tractography results. To compare the results of the effects of noise on the tractography algorithm, two steps are implemented as follows: 1) the data was mixed by Gaussian noise with a mean that correspond to the mean of the data (Figure 3 (a1 to c3)), and 2) distribution of noise is considered with zero means (Figure

3 (a4 to c4)).

Results for a Random noise

In Figure 4, the left column is the local phase tractography for mixed data by a random noise; the ordinary tractography results are shown in the right column.

Discussion

In the current study, the innovative idea is to consider the local image structures to find

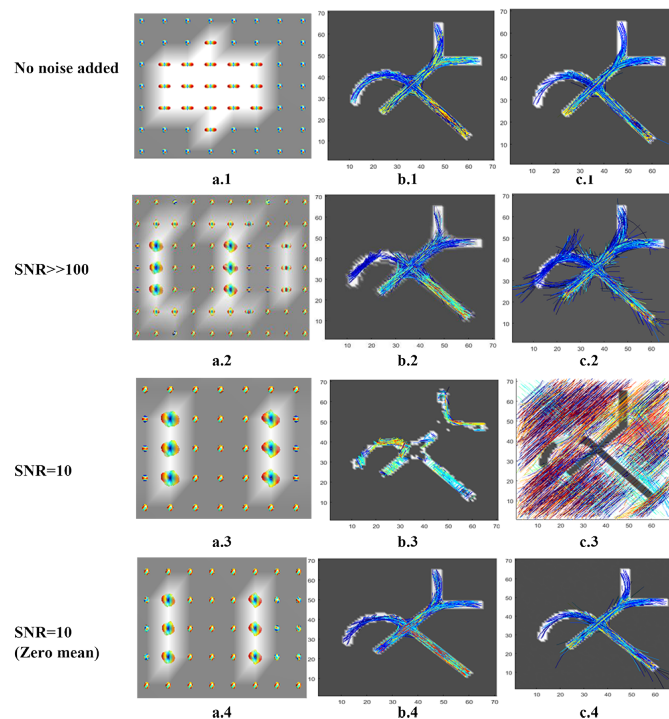


Figure 3: Gaussian noise added to the digital phantom. The Orientation distribution function (ODF) of digital phantom (left), Local phase tractography (middle), and Ordinary tractography (right)

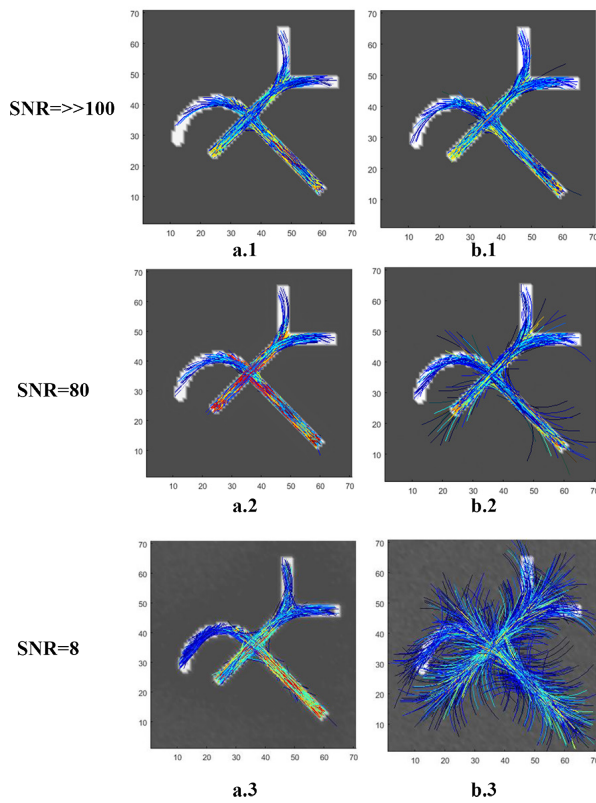


Figure 4: Random noise added to the digital phantom. Local phase tractography (left) and Ordinary tractography (right)

the main directions of the tractography algorithm without any post-process results of the tractography since only the pixels are selected as the input of the tractography algorithm that contains malicious information about the positions of the nerve fibers. Other methods used some manual techniques [13-16], such as determining a specific area on results of tractography to eliminate the area of interest and decreasing the false negative and false positive cases that the ROI was changed case by case whereas the proposed method automatically omits the pixels that are not a candidate to the tractography.

However, for diffusion signals with low intrinsic SNR, and in some cases, the noisy diffusion images, de-noising methods has a key role, in our proposed method, de-noising is not needed [24, 25] since the proposed innovative

algorithm is capable of separating noise from the main structures of the images, resulting in reducing the time of implementation of the algorithm.

Furthermore, the present study aimed to reduce the number of directions of gradients for image reconstruction for the first time in studies. The local phase features indicate changes in the gray level of the images, pixels, including more complex structures of images can reduce the number of ODF's. For an imaging sequence with the minimum gradients and calculated the main structures of the diffusion images, we used a better imaging sequence by using the local phase models.

One of the limitations of tractography algorithms of brain fibers is their unpredictability [6], related to the micrometers dimensions of fibers while the minimum dimension of an imaging voxel is not less than 0.5 mm. Based on the evidence, the proposed tractography algorithm should be more sensitive to the pixels of all directions to reduce the number of false-positive and false-negative cases [18]. Therefore, it is important to avoid getting stuck in pixels whose values may change due to noise [18]. The local phase features are good candidates to reduce misalignment tracts and tractography errors.

Conclusion

The local phase model of the diffusion images is presented based on designing a local mask; at the heart of our mask, a quadrature filter is embedded and the output of the mask is multiplied by the Fourier of diffusion images in all directions of the digital phantom. All directions of images are uniform with no distortions of noise in the data. Two types of noise were separately added to investigate the role of the local phase features on the tractography algorithm. The noise is considered with a distribution of Gaussian and random noise; the diffusion images were separately mixed by a distribution of Gaussian noise in two forms: a zero-mean noise and a noise with a mean of

data. Therefore, the tractography algorithm shows that the local phase features promote the efficiency of findings the configurations of fibers when the diffusion images are mixed with noise.

Acknowledgment

This research has been supported by the Tehran University of Medical Sciences & Health Services grant No. 38097.

Authors' Contribution

All authors contributed to the study's conception and design. AR. Shirazinodeh performed data collection and analysis. The first draft of the manuscript was written by AR. Shirazinodeh, H. Faraji, S. Sharifzadeh Javidi, AH. Jafari, MR. Nazemzadeh and HR. Salighehrad commented on previous versions of the manuscript. All the authors read, modified, and approved the final version of the manuscript.

Ethical Approval

The research was approved by the Institutional Ethical Committee of Tehran University of Medical Sciences (Approval code: (IR.TUMS.MEDICINE.REC.1398.771).

Informed consent

All experimental procedures were conducted according to the declaration of Helsinki; written informed consent was obtained from participants.

Funding

This project was supported by Tehran University of Medical Sciences Grant No. 38097.

Conflict of Interest

None

References

1. Basser PJ, Mattiello J, LeBihan D. MR diffusion tensor spectroscopy and imaging. *Biophys J*. 1994;66(1):259-67. doi: 10.1016/S0006-3495(94)80775-1. PubMed PMID: 8130344. PubMed PMCID: PMC1275686.
2. Tuch DS. Q-ball imaging. *Magn Reson Med*. 2004;52(6):1358-72. doi: 10.1002/mrm.20279. PubMed PMID: 15562495.
3. Wedeen VJ, Hagmann P, Tseng WY, Reese TG, Weisskoff RM. Mapping complex tissue architecture with diffusion spectrum magnetic resonance imaging. *Magn Reson Med*. 2005;54(6):1377-86. doi: 10.1002/mrm.20642. PubMed PMID: 16247738.
4. Tournier JD, Calamante F, Gadian DG, Connelly A. Direct estimation of the fiber orientation density function from diffusion-weighted MRI data using spherical deconvolution. *Neuroimage*. 2004;23(3):1176-85. doi: 10.1016/j.neuroimage.2004.07.037. PubMed PMID: 15528117.
5. Donahue CJ, Sotiropoulos SN, Jbabdi S, Hernandez-Fernandez M, et al. Using Diffusion Tractography to Predict Cortical Connection Strength and Distance: A Quantitative Comparison with Tracers in the Monkey. *J Neurosci*. 2016;36(25):6758-70. doi: 10.1523/JNEUROSCI.0493-16.2016. PubMed PMID: 27335406. PubMed PMCID: PMC4916250.
6. Daducci A, Dal Palú A, Descoteaux M, Thiran JP. Microstructure Informed Tractography: Pitfalls and Open Challenges. *Front Neurosci*. 2016;10:247. doi: 10.3389/fnins.2016.00247. PubMed PMID: 27375412. PubMed PMCID: PMC4893481.
7. Shirazinodeh A, Salighehrad H. Improving performance of tractography algorithm by using local phase features. In Proceedings of the 2021 ISMRM & SMRT; USA: ISMRM; 2021.
8. McNab JA, Polimeni JR, Wang R, Augustinack JC, Fujimoto K, et al. Surface based analysis of diffusion orientation for identifying architectonic domains in the in vivo human cortex. *Neuroimage*. 2013;69:87-100. doi: 10.1016/j.neuroimage.2012.11.065. PubMed PMID: 23247190. PubMed PMCID: PMC3557597.
9. Miller KL, Stagg CJ, Douaud G, Jbabdi S, Smith SM, Behrens TEJ, Jenkinson M, Chance SA, et al. Diffusion imaging of whole, post-mortem human brains on a clinical MRI scanner. *Neuroimage*. 2011;57(1):167-81. doi: 10.1016/j.neuroimage.2011.03.070. PubMed PMID: 21473920. PubMed PMCID: PMC3115068.
10. Sotiropoulos SN, Hernández-Fernández M, Vu AT, Andersson JL, Moeller S, Yacoub E, et al. Fusion in diffusion MRI for improved fibre orientation estimation: An application to the 3T and 7T data of the Human Connectome Project. *Neuroimage*. 2016;134:396-409. doi: 10.1016/j.neuroimage.2016.04.014. PubMed PMID: 27071694. PubMed PMCID: PMC6318224.
11. Uğurbil K, Xu J, Auerbach EJ, Moeller S, Vu AT, Duarte-Carvajalino JM, Lenglet C, Wu X, Schmitter S, et al. Pushing spatial and temporal resolution for

- functional and diffusion MRI in the Human Connectome Project. *Neuroimage*. 2013;**80**:80-104. doi: 10.1016/j.neuroimage.2013.05.012. PubMed PMID: 23702417. PubMed PMCID: PMC3740184.
12. Ma X, Uğurbil K, Wu X. Denoise magnitude diffusion magnetic resonance images via variance-stabilizing transformation and optimal singular-value manipulation. *Neuroimage*. 2020;**215**:116852. doi: 10.1016/j.neuroimage.2020.116852. PubMed PMID: 32305566. PubMed PMCID: PMC7292796.
 13. McGibney G, Smith MR. An unbiased signal-to-noise ratio measure for magnetic resonance images. *Med Phys*. 1993;**20**(4):1077-8. doi: 10.1118/1.597004. PubMed PMID: 8413015.
 14. Sijbers J, Den Dekker AJ, Van Dyck D, Raman E. Estimation of signal and noise from Rician distributed data. In Proceedings of the International Conference on Signal Processing and Communications; Canaria, Spain; 1998. p. 140-2.
 15. Aja-Fernandez S, Alberola-Lopez C, Westin CF. Noise and signal estimation in magnitude MRI and Rician distributed images: a LMMSE approach. *IEEE Trans Image Process*. 2008;**17**(8):1383-98. doi: 10.1109/TIP.2008.925382. PubMed PMID: 18632347.
 16. Wiest-Daesslé N, Prima S, Coupé P, Morrissey SP, Barillot C. Rician noise removal by non-Local Means filtering for low signal-to-noise ratio MRI: applications to DT-MRI. *Med Image Comput Comput Assist Interv*. 2008;**11**(Pt 2):171-9. doi: 10.1007/978-3-540-85990-1_21. PubMed PMID: 18982603. PubMed PMCID: PMC2665702.
 17. Eichner C, Cauley SF, Cohen-Adad J, Möller HE, Turner R, Setsompop K, Wald LL. Real diffusion-weighted MRI enabling true signal averaging and increased diffusion contrast. *Neuroimage*. 2015;**122**:373-84. doi: 10.1016/j.neuroimage.2015.07.074. PubMed PMID: 26241680. PubMed PMCID: PMC4651971.
 18. Campbell JS, Pike GB. Potential and limitations of diffusion MRI tractography for the study of lan-
guage. *Brain Lang*. 2014;**131**:65-73. doi: 10.1016/j.bandl.2013.06.007. PubMed PMID: 23910928.
 19. Poupon C, Rieul B, Kezele I, Perrin M, Poupon F, Mangin JF. New diffusion phantoms dedicated to the study and validation of high-angular-resolution diffusion imaging (HARDI) models. *Magn Reson Med*. 2008;**60**(6):1276-83. doi: 10.1002/mrm.21789. PubMed PMID: 19030160.
 20. Aganj I, Lenglet C, Jahanshad N, Yacoub E, Harel N, Thompson PM, Sapiro G. A Hough transform global probabilistic approach to multiple-subject diffusion MRI tractography. *Med Image Anal*. 2011;**15**(4):414-25. doi: 10.1016/j.media.2011.01.003. PubMed PMID: 21376655. PubMed PMCID: PMC3115463.
 21. Felsberg M, Sommer G. The monogenic signal. *IEEE Transactions on Signal Processing*. 2001;**49**(12):3136-44. doi: 10.1109/78.969520.
 22. Unser M, Sage D, Van De Ville D. Multiresolution monogenic signal analysis using the Riesz-Laplace wavelet transform. *IEEE Trans Image Process*. 2009;**18**(11):2402-18. doi: 10.1109/TIP.2009.2027628. PubMed PMID: 19605325.
 23. Leemans A, Sijbers J, Verhoye M, Van Der Linden A, Van Dyck D. Mathematical framework for simulating diffusion tensor MR neural fiber bundles. *Magn Reson Med*. 2005;**53**(4):944-53. doi: 10.1002/mrm.20418. PubMed PMID: 15799061.
 24. Fadnavis S, Batson J, Garyfallidis E. Patch2Self: Denoising Diffusion MRI with Self-Supervised Learning. 34th Conference on Neural Information Processing Systems; Vancouver, Canada: NeurIPS; 2020.
 25. Moeller S, Pisharady PK, Ramanna S, Lenglet C, Wu X, Dowdle L, Yacoub E, Uğurbil K, Akçakaya M. NOise reduction with Distribution Corrected (NORDIC) PCA in dMRI with complex-valued parameter-free locally low-rank processing. *Neuroimage*. 2021;**226**:117539. doi: 10.1016/j.neuroimage.2020.117539. PubMed PMID: 33186723. PubMed PMCID: PMC7881933.